TABLE II
PSNR VALUES OBTAINED BY THE ORIGINAL DVQ [4] AND THE PROPOSED

	1.5 bpp		1.75 bpp		2 bpp	
	DVQ [4]	proposed	DVQ [4]	proposed	DVQ [4]	proposed
airplane	36.26	37.41	37.80	38.84	39.27	40.28
baboon	29.29	29.93	30.78	31.40	31.88	32.54
peppers	35.85	36.99	37.41	38.26	38.84	39.74
sailboat	33.77	34.75	35.25	36.12	36.61	37.41
lenna	34.53	35.60	35.96	36.96	37.41	38.54

with the training set composed by five images. Each codebook was designed using a centroid condition consistent with the respective distortion measure used in the codebook search. The results obtained by the DVQ system [4], that uses (10), and by the implementation using (11) are shown in Table II. This table shows the PSNR values in dB for various bit rates, which is defined by PSNR $= 10\log_{10}$ (255^2/MSE). The bit rates are calculated as $\log_2 M$, where M is the number of codewords (no entropy coding was performed). All the images cited in this comparison did not belong to the training set. Table II shows that the proposed modification on the distortion measure allows the PSNR to increase 1 dB for the Lenna image. As commented previously, these results are only presented to validate the proposed structure.

IV. CONCLUSION

In this correspondence, a new PVQ structure is proposed. This PVQ scheme uses different scalar predictors in the encoding and decoding processes. The discrepancy between the predictions made in the encoding and in decoding is compensated by the vector quantizer stage that uses a consistent distortion measure. The centroid condition for the proposed distortion measure was described.

To validate the method, it was suggested a modification on an image coding system [4] that already used different predictors in the encoding and decoding processes. This modification led to an improvement of 1 dB in PSNR for the Lenna image.

REFERENCES

[1] A. Gersho and R. M. Gray, *Vector Quantization and Signal Compression.* Norwell, MA: Kluwer, 1992.

[2] V. Cuperman and A. Gersho, "Adaptive differential vector coding of speech," in *Proc. IEEE GLOBECOM*, Miami, FL, Dec. 1982, pp. 1092–1096.

[3] C. W. Rutledge, "Vector DPCM: Vector predictive coding of color images," in *Proc. IEEE GLOBECOM*, Sept. 1986, pp. 1158–1164.

[4] J. Fowler, M. Carbonara, and S. Ahalt, "Image coding using differential vector quantization," *IEEE Trans. Circuits Syst. Video Technol.*, vol. 3, pp. 350–367, Oct. 1993.

[5] P. Cosman, R. Gray, and M. Vetterli, "Vector quantization of images subbands: A survey, " *IEEE Trans. Image Processing*, vol. 5, pp. 202–225, Feb. 1996.

[6] S. Rizvi, L.-C. Wang, and N. Nasrabadi, "Nonlinear vector prediction using feed-forward neural networks," *IEEE Trans. Image Processing*, vol. 6, pp. 1431–1436, Oct. 1997.

[7] H.-M. Hang and J. Woods, "Predictive vector quantization of images," *IEEE Trans. Commun.*, vol. 33, pp. 1208–1219, Nov. 1985.

[8] B. Vasudev, "Predictive VQ schemes for grayscale image compression," in *Proc. IEEE GLOBECOM*, 1987, pp. 11.8.1–11.8.6.

[9] J. Modestino and Y. Kim, "Adaptive entropy-coded predictive vector quantization of images," *IEEE Trans. Signal Proc.*, vol. 40, pp. 633–644, Mar. 1992.

[10] USC Image Database. Univ. Southern Calif., Signal and Image Processing Inst., Los Angeles, CA.

[11] V. Cuperman and A. Gersho, "Vector predictive coding of speech at 16 kbits/s," *IEEE Trans. Commun.*, vol. COMM-33, pp. 685–696, July 1985.

Blind Image Deconvolution Using a Robust GCD Approach

S. Unnikrishna Pillai and Ben Liang

***Abstract*— In this correspondence, a new viewpoint is proposed for estimating an image from its distorted versions in presence of noise without the *a priori* knowledge of the distortion functions. In z-domain, the desired image can be regarded as the greatest common polynomial divisor among the distorted versions. With the assumption that the distortion filters are finite impulse response (FIR) and relatively coprime, in the absence of noise, this becomes a problem of taking the greatest common divisor (GCD) of two or more two-dimensional (2-D) polynomials. Exact GCD is not desirable because even extremely small variations due to quantization error or additive noise can destroy the integrity of the polynomial system and lead to a trivial solution. Our approach to this blind deconvolution approximation problem introduces a new robust interpolative 2-D GCD method based on a one-dimensional (1-D) Sylvester-type GCD algorithm. Experimental results with both synthetically blurred images and real motion-blurred pictures show that it is computationally efficient and moderately noise robust.**

***Index Terms*—Blind image deconvolution, equalization, image processing.**

I. INTRODUCTION

In many problems including communication, satellite imaging, and synthetic aperture radar (SAR), the output observation consists of a desired input that has been distorted by a blurring function such as camera motion. In communication scenes, for example, the output is the convolution of an input data stream and the channel impulse response, both of which are unknown. Similarly, in ordinary blurred images, the final picture can be represented as the result of convolution between the desired picture and a blurring function that will result from camera motion and/or slow shutter speed. In all these situations, blind identification consists of determining the input function and blurring or channel transfer functions from the output observation. For example, with $x(n)$ representing the input to a channel with impulse response $h(n)$, the output can be represented as $y(n) = x(n) * h(n)$. Taking z-transforms on both sides, we get

$$Y(z) = X(z)H(z) \tag{1}$$

Manuscript received March 28, 1997; revised June 19, 1998. This research work was supported by the Office of Naval Research under Contract N-00014-89-J-1512P-5. The associate editor coordinating the review of this manuscript was Prof. Stephen E. Reichenbach.

S. U. Pillai is with the Department of Electrical Engineering, Polytechnic University, Brooklyn, NY 11201 USA (e-mail: pillai@ee.poly.edu; pillai@fire.poly.edu).

B. Liang was with the Department of Electrical Engineering, Polytechnic University, Brooklyn, NY 11201 USA. He is now with the Electrical Engineering Department, Cornell University, Ithaca, NY 14852 USA.

Publisher Item Identifier S 1057-7149(99)00931-8.

where $x(n) \leftrightarrow X(z)$, $h(n) \leftrightarrow H(z)$, and $y(n) \leftrightarrow Y(z)$ represent the corresponding z-transform pairs. It is clear that from a knowledge of the output $Y(z)$ alone, it is impossible to obtain $X(z)$ and $H(z)$ separately. On the other hand, usually only the output information is available, and that makes the blind identification problem more challenging. Clearly, in addition to $Y(z)$, some additional information about either the input or channel characteristics is required to successfully solve this problem. The same formulation applies in the case of blurred images also.

To see this, let $p(i,j)$ represent the desired image, $d(i,j)$ the blurring function, and $n(i,j)$ additive noise. Letting $f(i,j)$ represent the blurred image, we have

$$f(i,j) = p(i,j) * d(i,j) + n(i,j). \tag{2}$$

Using the two-dimensional (2-D) z-transforms, (2) reduces to

$$F(z_1,z_2) = P(z_1,z_2)D(z_1,z_2) + N(z_1,z_2) \tag{3}$$

where $f(i,j) \leftrightarrow F(z_1,z_2)$, $p(i,j) \leftrightarrow P(z_1,z_2)$, $d(i,j) \leftrightarrow D(z_1,z_2)$, and $n(i,j) \leftrightarrow N(z_1,z_2)$. Such a model is applicable in all scenarios where the distortion can be modeled as a linear filter acting on the original image. For example, camera motion, intermediate medium in satellite photography, can all be modeled as in (2) and (3). Once again it is clear from (3) that even in the absence of noise, knowing the blurred picture $F(z_1,z_2)$ alone is not sufficient in general to obtain either the original image or the blurring function.

Blind image deconvolution is the process of identifying both the true image and the blurring function from the degraded image, using partial information about the imaging system. This process is critical because in many practical situations, unlike classical linear image restoration techniques, the blur function is often unknown. In some applications, such as astronomy and x-ray imaging, it is often costly to obtain *a priori* information about the imaged scene and the distortion, and in others, such as real-time video conferencing, it is simply impossible to predetermine the parameters of the blurring function.

Tempting as blind deconvolution from a single blurred image may seem, it is often *ill-posed*. A small amount of additive noise can lead to large deviations, and a unique solution may not be found. In existing methods dealing with such problems, reliability is often achieved at the expense of high computational complexity.

Many techniques have been proposed in the past to identify the blurring function and the original image [1]–[12]. Among them, *a priori* blur identification methods perform blind deconvolution by identifying the blurring function prior to restoration. The most popular among them make use of the frequency domain nulls of the degraded image to perform blind deconvolution by partitioning the blurred image in (2) into smaller frames, each of which is large enough to contain the blurring function. This method assumes that the true image possibly contains edges or point sources, and that the blurring function is symmetric and nonminimum phase with a possibly known parametric form. The method of zero sheet separation proposed by Lane and Bates [2] is the most direct way of blind deconvolution as it tries to exploit the irreducible property present in most of the 2-D polynomials. In the absence of noise, assuming that both the polynomials $P(z_1,z_2)$ and $D(z_1,z_2)$ in (3) are irreducible and possess distinct zero sheets, the feasibility of this approach was proved by Lane and Bates and demonstrated by Bones [3]. Although computationally complex, Ghiglia has given a systematic approach of this method [4]. This algorithm is highly sensitive to noise, and has a computational complexity of $O(n^8)$, for an $n \times n$ image.

Other methods to deconvolve a blurred image include autoregressive moving average (ARMA) modeling [5]–[7], the simulated annealing (SA) algorithm [8], the nonnegativity and support constraints recursive inverse filtering (NAS-RIF) algorithm [9], as well as nonparametric methods based on higher order statistics [10].

When multiple blurred versions of the same scene are available, inspired by the subspace channel equalization methods in the communication scenario [13], blind deconvolution is considered in [11] and [12]. The subspace technique presented in [11] is similar to an extension of our one-dimensional (1-D) Sylvester-type algorithm, as shown in the next section, which leads to extremely high computational complexity and memory storage requirements. A finite impulse response (FIR) multichannel equalization scheme is proposed in [12] utilizing multiple blurred images whose 2-D blurring functions in the z-domain have no common zeros. More than four blurred images of the same scene are needed in this case.

Our approach to the blind deblurring problem makes use of a fresh perspective of polynomial GCD approximation. Let $d_1(i,j)$ and $d_2(i,j)$ represent two *distinct* blurring functions with z-transforms $D_1(z_1,z_2)$ and $D_2(z_1,z_2)$, respectively. Further, let $f_1(i,j)$ and $f_2(i,j)$ represent the corresponding blurred outputs. Then

$$f_k(i,j) = p(i,j) * d_k(i,j), \qquad k = 1,2. \tag{4}$$

In z-domain, (4) translates to

$$F_k(z_1,z_2) = P(z_1,z_2)D_k(z_1,z_2), \qquad k = 1,2 \tag{5}$$

where $f_k(i,j) \leftrightarrow F_k(z_1,z_2)$.

From (5), if the two distortion transfer functions $D_1(z_1,z_2)$ and $D_2(z_1,z_2)$ are relatively co-prime, $P(z_1,z_2)$ is the greatest common divisor (GCD) of $F_1(z_1,z_2)$ and $F_2(z_1,z_2)$, i.e., if

$$\mathrm{GCD}\{D_1(z_1,z_2), D_2(z_1,z_2)\} = 1 \tag{6}$$

then

$$\mathrm{GCD}\{F_1(z_1,z_2), F_2(z_1,z_2)\} = P(z_1,z_2). \tag{7}$$

Equation (7) can be used to recover the original image $p(i,j)$ from the distorted versions $f_1(i,j)$ and $f_2(i,j)$. Note that (6) represents the necessary and sufficient condition for the recovery of the original image from its distinct blurred versions without the actual knowledge of the blurring functions.

Observe that $D_1(z_1,z_2)$ and $D_2(z_1,z_2)$ need not be free of common zeros, a much more restrictive (and unnecessary) assumption. However, if such is the case, then from Bezout's identity, there exist two other polynomial functions $E_1(z_1,z_2)$ and $E_2(z_1,z_2)$ such that [14]

$$D_1(z_1,z_2)E_1(z_1,z_2) + D_2(z_1,z_2)E_2(z_1,z_2) = 1 \tag{8}$$

and the deblurring can be performed in the FIR domain. Apparently, for two (or more) variable polynomials, absence of common zeros is an exception rather than the rule.[1] However, since the GCD procedure does permit common zeros between the blurring functions, it represents a much more general framework for deblurring.

Although the above formulation requires two distinct blurred images, it is important to realize that often such information can be extracted from a single frame itself. For example, referring back to the model in (2)–(3), assume that the blurring function $d(i,j)$ has a much smaller support size compared to the image. If we restrict our attention to two nonoverlapping regions R_1 and R_2 that are large enough to contain the blurring function and sufficiently far apart within the support of $f(i,j)$, we may write (ignoring noise)

$$f_k(i,j) = p_k(i,j) * d(i,j), \qquad p_k(i,j) \in R_k, \quad k = 1,2. \tag{9}$$

[1]Even the simplest two-variable polynomials $D_1(z_1,z_2) = z_1$ and $D_2(z_1,z_2) = z_2$ have a common zero at (0, 0). However, they are relatively factor co-prime.

Clearly, their transforms can be expressed as in (5), and if $P_1(z_1, z_2)$ and $P_2(z_1, z_2)$ are relatively co-prime, the above GCD procedure can be used to extract the blurring transfer function $D(z_1, z_2)$ from a single frame itself.

Unfortunately, the existing two-variable GCD algorithms, such as those used in the commercial programs Matlab and Maple, are extremely sensitive to quantization noise, and a direct application of the GCD algorithm will invariably fail. For practical considerations, the effect of quantization needs to be addressed, as it leads to systematic coefficient error. In addition, one may not have the luxury of obtaining distinct distorted multiple versions of the same image. In reality, as in a picture taken with a shaken camera, one may only have a *single* version of a distorted picture, and the problem is to obtain the original image in this situation.

In this context, our approach to the blind image deconvolution problem in presence of noise is outlined in the next section as the estimation of the "best" GCD of 2-D polynomials.

II. A New Blind Deconvolution/Deblurring Algorithm

Let $f_1(m, n)$ and $f_2(m, n)$ represent two distorted versions of a true image $p(m, n)$. From (4), with $n_k(m, n) \leftrightarrow N_k(z_1, z_2)$ representing the noise, we have

$$F_k(z_1, z_2) = P(z_1, z_2)D_k(z_1, z_2) + N_k(z_1, z_2), \quad k = 1, 2. \tag{10}$$

When $N_1(z_1, z_2) = N_2(z_1, z_2) = 0$, we can easily see that the original image can be reconstructed as the GCD of $F_1(z_1, z_2)$ and $F_2(z_1, z_2)$, provided that $D_1(z_1, z_2)$ and $D_2(z_1, z_2)$ are relatively co-prime [14]. However, even under such noiseless conditions, direct GCD implementation of $F_1(z_1, z_2)$ and $F_2(z_1, z_2)$ using symbolic mathematical tools such as Maple often leads to a trivial solution due to the high sensitivity of the existing 2-D GCD methods.

When there is noise, $P(z_1, z_2)$ only approximates as the common factor that divides $F_1(z_1, z_2)$ and $F_2(z_1, z_2)$. In this context, the technique described below makes use of an interesting 1-D formulation and then uses a least square approach to obtain the best estimate for $P(z_1, z_2)$.

To begin with, we will examine the 1-D Sylvester-type algorithm [14] that will turn out to be useful to our present discussion. Let

$$A(z) = a_0 + a_1 z + a_2 z^2 + \cdots + a_n z^n \tag{11}$$

$$B(z) = b_0 + b_1 z + b_2 z^2 + \cdots + b_m z^m \tag{12}$$

be two polynomials of degrees n and m, respectively, with their GCD equal to $P(z)$. Suppose $P(z)$ is of degree $r \geq 1$. Then

$$\frac{A(z)}{C(z)} = \frac{B(z)}{D(z)} = P(z) \tag{13}$$

where

$$C(z) = c_0 + c_1 z + c_2 z^2 + \cdots + c_{n-r} z^{n-r} \tag{14}$$

and

$$D(z) = d_0 + d_1 z + d_2 z^2 + \cdots + d_{m-r} z^{m-r} \tag{15}$$

are two polynomials that are relatively co-prime. It follows that

$$A(z)D(z) - B(z)C(z) = 0 \tag{16}$$

and by equating the coefficients of like powers of z on both sides of (16), it has the matrix equivalence of

$$S\boldsymbol{x} = \mathbf{0} \tag{17}$$

where

$$\boldsymbol{x} = [d_{m-r}, \cdots, d_2, d_1, d_0, -c_0, -c_1, -c_2, \cdots, -c_{n-r}] \tag{18}$$

and S is given by

$$S \triangleq \begin{bmatrix} a_n & a_{n-1} & \cdots & & a_1 & a_0 & 0 & \cdots & 0 \\ 0 & a_n & a_{n-1} & \cdots & & a_1 & a_0 & \cdots & 0 \\ \vdots & & \vdots & & & & & & \vdots \\ 0 & \cdots & 0 & a_n & a_{n-1} & \cdots & & a_1 & a_0 \\ 0 & 0 & \cdots & 0 & b_m & b_{m-1} & \cdots & b_1 & b_0 \\ 0 & \cdots & 0 & b_m & b_{m-1} & \cdots & b_1 & b_0 & 0 \\ \vdots & & & & \vdots & & \vdots & & \vdots \\ b_m & b_{m-1} & \cdots & & b_1 & b_0 & 0 & \cdots & 0 \end{bmatrix}. \tag{19}$$

The matrix S has $n + m - 2r + 2$ rows and $n + m - r + 1$ columns, and to find $\boldsymbol{x}$, if r is known, we may perform singular value decomposition on S. Since $C(z)$ and $D(z)$ are two unique polynomials of degrees $n - r$ and $m - r$, respectively, it follows that x has a unique solution in (17), and consequently S must posses $n + m - 2r + 1$ linearly independent rows. As a result, the singular vector that corresponds to the zero singular value of S is the least square solution of (17) for $\boldsymbol{x}$, and it contains the coefficient values of $C(z)$ and $D(z)$.

If r is not known, the situation is more complicated, since it is not even possible to form S. However, in that case, (17) can be rewritten as

$$\boldsymbol{x}_0 S_0 = 0 \tag{20}$$

where

$$\boldsymbol{x}_0 = [d_{m-1}, \cdots, d_2, d_1, d_0, -c_0, -c_1, -c_2, \cdots, -c_{n-1}] \tag{21}$$

with

$$d_{m-1} = \cdots = d_{m-r+1} = c_{n-r+1} = \cdots = c_{n-1} = 0 \tag{22}$$

and S_0 given by the standard Sylvester (resultant) matrix

$$S_0 = \begin{bmatrix} a_n & a_{n-1} & \cdots & & a_1 & a_0 & 0 & \cdots & 0 \\ 0 & a_n & a_{n-1} & \cdots & & a_1 & a_0 & \cdots & 0 \\ \vdots & & \vdots & & & & & & \vdots \\ 0 & \cdots & 0 & a_n & a_{n-1} & \cdots & & a_1 & a_0 \\ 0 & 0 & \cdots & 0 & b_m & b_{m-1} & \cdots & b_1 & b_0 \\ 0 & \cdots & 0 & b_m & b_{m-1} & \cdots & b_1 & b_0 & 0 \\ \vdots & & & & \vdots & & \vdots & & \vdots \\ b_m & b_{m-1} & \cdots & & b_1 & b_0 & 0 & \cdots & 0 \end{bmatrix} \tag{23}$$

of size $(n + m) \times (n + m)$.

Interestingly, the necessary and sufficient condition for the polynomials $A(z)$ and $B(z)$ in (11)–(12) to have a nonconstant GCD is that the resultant Sylvester matrix S_0 in (23) be singular [14]. In particular, if the GCD is of degree r, then (20) must reduce to (17), and because of the unique nature of the polynomials $C(z)$ and $D(z)$ and their degree restrictions, it follows that associated with the singular value zero, S_0 must have a singular vector exhibiting the restrictions in (22) for its peripheral coefficients.

The rank of S_0 can be inferred by noticing the structural relationship between S and S_0:

$$S_0 = \begin{bmatrix} & r-1 \text{ rows} & \\ & S & \\ r-1 \text{ columns} & & \\ & r-1 \text{ rows} & \end{bmatrix}. \tag{24}$$

From (24), since S_0 is obtained by adding an additional $r-1$ columns to the column matrix containing S, to start with its rank can at most be $n+m-r$. However by taking the structure in (22) into account, it follows that S_0 is of rank $n+m-r$, provided $a_n \neq 0$ and $b_m \neq 0$. The above discussion suggests that of the various singular vectors that correspond to the singular value zero for S_0, the one that satisfies (22) for the largest value of r represents the desired solution.

Alternatively, referring back to (23) and (24), let S_k denote the submatrix of size $(n+m-2k)\times(n+m-k)$ obtained by striking out the first k and last k rows of S_0, and the first k columns of S_0. Note that S_{r-1} is the same as S in (19). The degree of the GCD polynomial $P(z)$ can be characterized in terms of these submatrices.

Lemma: Let $\mathrm{GCD}\{A(z), B(z)\} = P(z)$ with degree $P(z) = r$. Then $S_0, S_1, \cdots, S_{r-1}$ are singular, and S_{r-1} is of rank $n+m-2r+1$.

The above lemma indicates a new procedure to obtain r, and knowing r one may go back to (17) to obtain $C(z)$ and $D(z)$. $P(z)$ can then be found from (13) up to a constant scalar factor.

In the presence of noise, S_0 in general has full rank, i.e., the singular values of S_0 are all greater than zero. In this case, we can approximate the rank of the noiseless S_0 by setting the small singular values to zero. This procedure works well under low to moderate (SNR $\geq$ 30 dB) noise contamination. Note that even if the size of the blurring function is not exactly determined, knowing its approximate range is usually enough. Due to the low complexity of the proposed algorithm, as shown here and later for the 2-D case, we can carry out a few blur size estimations and find the best image restoration by visual inspection or certain parametric determination procedure according to the known image characteristics.

Long division should be avoided in (13), because in doing so numerical error would propagate and accumulate toward the lower degree coefficients, and when the dividend is a high order polynomial, the last terms of the quotient would be inaccurate. Instead, we first take the N-point Fourier transform on the two vectors, where N is the length of the vector corresponding to the dividend, then divide through the resulting vectors element by element, which leads to the N-point Fourier transform of the coefficient vector of the desirable quotient of polynomials.

Although it is possible to directly extend the technique described above in (11)–(23) to the 2-D case in terms of constant matrices generated from the given 2-D polynomial coefficients, this direct procedure leads to prohibitively large size matrices. For example, for images of size $N\times N$, the matrix corresponding to (19) will be of size $2N^2\times 2N^2$. Since computations involved in a matrix singular value decomposition (SVD) are proportional to the cube of the matrix size, this direct procedure requires operations of the order of $O(N^6)$ for SVD alone [15]–[17]. This is clearly an impossible task even for moderate value of N. In this context, we will describe how the 1-D GCD algorithm can be used in the 2-D blind deconvolution problem in a computationally efficient manner.

We assume that the two blurred images $f_1(m,n)$ and $f_2(m,n)$ of the original image $p(m,n)$ are both $M\times N$ matrices. Obviously, the elements of these matrices are the coefficients of the z-transforms of the respective images. Using a conventional discrete Fourier transform least squares (CDFT-LS) approach [4], [3], we substitute $z_1 = e^{-j(2\pi m/M)}$, $m = 0, 1, \cdots, M-1$, into both $F_1(z_1, z_2)$ and $F_2(z_1, z_2)$. For each m, this results in two 1-D polynomials

$$F_k(e^{-j(2\pi m/M)}, z_2) = P(e^{-j(2\pi m/M)}, z_2) D_k(e^{-j(2\pi m/M)}, z_2), \quad k = 1, 2. \tag{25}$$

Notice that $P(e^{-j(2\pi m/M)}, z_2)$ is still a common factor of $F_1(e^{-j(2\pi m/M)}, z_2)$ and $F_2(e^{-j(2\pi m/M)}, z_2)$, except that in this case the polynomials involved are in one variable, z_2, only. Thus the 1-D GCD algorithm yields the scaled quantity $c_0(e^{-j(2\pi m/M)})P(e^{-j(2\pi m/M)}, z_2)$. To proceed further, for each value of m we further substitute $z_2 = e^{-j(2\pi n/N)}$, $n = 0, 1, \cdots, N-1$, in this GCD and form a matrix of discrete Fourier transform elements

$$A(m,n) = c(m)P(e^{-j(2\pi m/M)}, e^{-j(2\pi n/N)}) \tag{26}$$

scaled in each row by a constant $c(m) = c_0(e^{-j(2\pi m/M)})$. Although in general $c_0(e^{-j(2\pi m/M)})$ is also a function of z_2, as shown below, its dependence on z_2 only occurs at a finite set of points, and this justifies the above representation independent of z_2. To reduce the numerical error, in the following computation, we rewrite (26) as

$$A(m,n)a(m) = P(e^{-j(2\pi m/M)}, e^{-j(2\pi n/N)}). \tag{27}$$

Carrying out similar operations by substituting $z_2 = e^{-j(2\pi n/N)}$ in $F_1(z_1, z_2)$ and $F_2(z_1, z_2)$, taking their 1-D GCD and further substituting $z_1 = e^{-j(2\pi m/M)}$, we obtain another matrix, $B(m,n)$, which is related to the discrete Fourier transform of the original image by columnwise scaling

$$B(m,n)b(n) = P(e^{-j(2\pi m/M)}, e^{-j(2\pi n/N)}). \tag{28}$$

From (27) and (28) we have

$$A(m,n)a(m) - B(m,n)b(n) = 0. \tag{29}$$

This equation set has the matrix equivalence of

$$\boldsymbol{\Gamma}\boldsymbol{y} = \mathbf{0} \tag{30}$$

where

$$\boldsymbol{y} \triangleq [a(1), a(2), \cdots, a(M), b(1), b(2), \cdots, b(N)]^T \tag{31}$$

and (32), shown at the bottom of the next page. Equation (30) is overdetermined, and multiplying by $\boldsymbol{\Gamma}^T$ on both sides, we get

$$\boldsymbol{\Gamma}^T\boldsymbol{\Gamma}\boldsymbol{y} = \mathbf{0}. \tag{33}$$

We may solve (33) in a least-squares sense by considering the equation

$$\boldsymbol{\Gamma}^T\boldsymbol{\Gamma}\boldsymbol{z} = \lambda\boldsymbol{z} \tag{34}$$

for the eigenvector $\boldsymbol{z}$ corresponding to the smallest eigenvalue of $\boldsymbol{\Gamma}^T\boldsymbol{\Gamma}$. Using (31) so obtained, the estimated Fourier transform of the original image is then calculated by

$$P(e^{-j(2\pi m/M)}, e^{-j(2\pi n/N)}) = \tfrac{1}{2}[A(m,n)a(m) + B(m,n)b(n)]. \tag{35}$$

Finally, the inverse Fourier transform of (35) yields an estimate of the original image. It is interesting to note that for images of

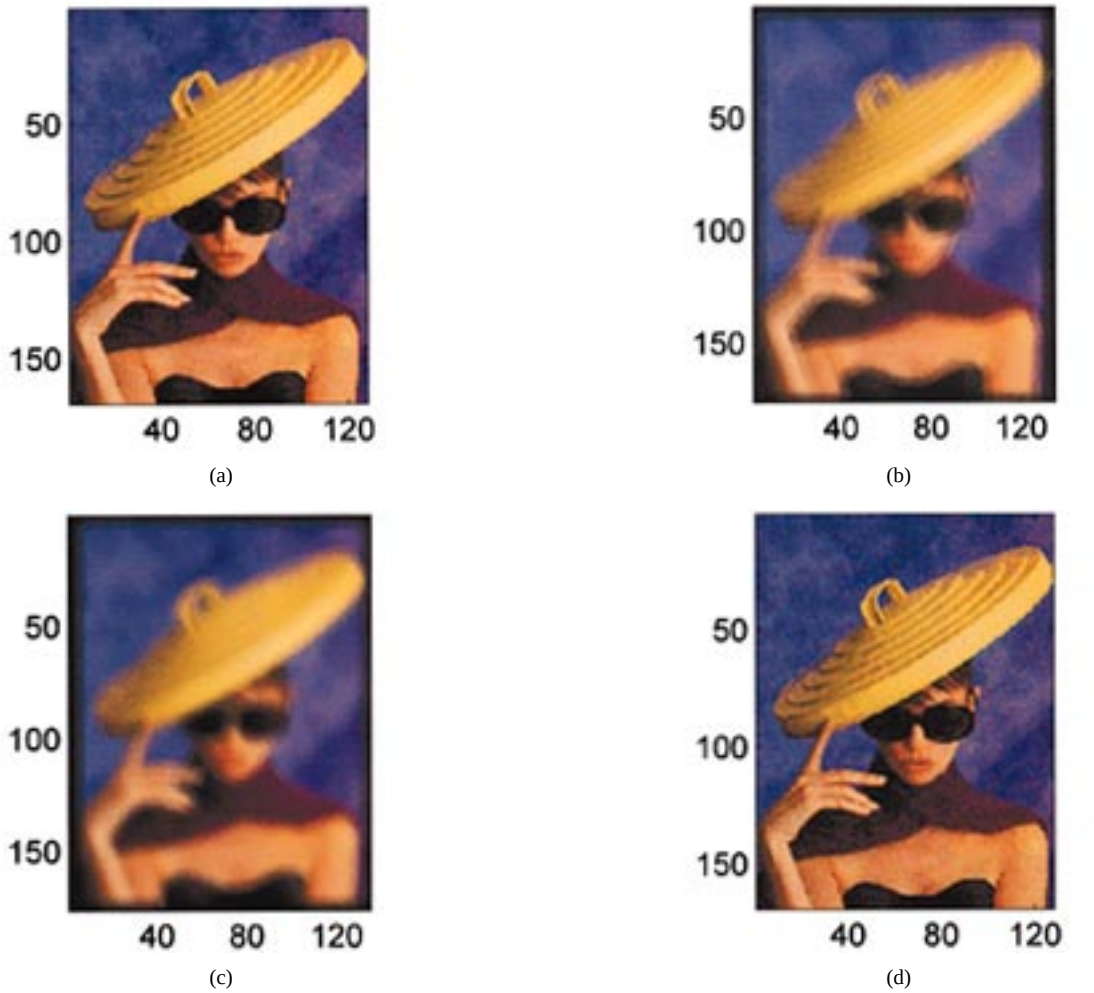

Fig. 1. Blind deblurring from two distorted and noisy (SNR = 45 dB) images. (a) Original image. (b)–(c) Distorted Images. (d) Reconstructed Image.

size $N \times N$, this algorithm only requires $O(N^4)$ computations, a substantial saving compared to the direct Sylvester-type procedure.

The method described above can be rigorously established by incorporating an important property of relatively co-prime polynomials. To see this, let $D_1(z_1, z_2)$ and $D_2(z_1, z_2)$ be two relatively co-prime polynomials. In that case, from standard theory, there exist two other polynomials $A_1(z_1, z_2)$ and $A_2(z_1, z_2)$ such that [14]

$$D_1(z_1, z_2)A_1(z_1, z_2) + D_2(z_1, z_2)A_2(z_1, z_2) = \psi_1(z_1) \not\equiv 0 \tag{36}$$

$$\boldsymbol{\Gamma} \triangleq \begin{bmatrix}
A(1,1) & 0 & \cdots & 0 & -B(1,1) & 0 & \cdots & 0 \\
A(1,2) & 0 & \cdots & 0 & 0 & -B(1,2) & \cdots & 0 \\
A(1,3) & 0 & \cdots & 0 & 0 & 0 & \cdots & 0 \\
\cdots & \cdots & \cdots & \cdots & \cdots & \cdots & \cdots & \cdots \\
A(1,N) & 0 & \cdots & 0 & 0 & 0 & \cdots & -B(1,N) \\
0 & A(2,1) & \cdots & 0 & -B(2,1) & 0 & \cdots & 0 \\
0 & A(2,2) & \cdots & 0 & 0 & -B(2,2) & \cdots & 0 \\
0 & A(2,3) & \cdots & 0 & 0 & 0 & \cdots & 0 \\
\cdots & \cdots & \cdots & \cdots & \cdots & \cdots & \cdots & \cdots \\
0 & A(2,N) & \cdots & 0 & 0 & 0 & \cdots & -B(2,N) \\
\vdots & \vdots & & \vdots & \vdots & \vdots & & \vdots \\
0 & 0 & \cdots & A(M,1) & -B(M,1) & 0 & \cdots & 0 \\
0 & 0 & \cdots & A(M,2) & 0 & -B(M,2) & \cdots & 0 \\
0 & 0 & \cdots & A(M,3) & 0 & 0 & \cdots & 0 \\
\cdots & \cdots & \cdots & \cdots & \cdots & \cdots & \cdots & \cdots \\
0 & 0 & \cdots & A(M,N) & 0 & 0 & \cdots & -B(M,N)
\end{bmatrix} \tag{32}$$

(a) Blurred Image (Moving Truck on BQE; Early April 97)

(b) Image Magnitude After GCD Processing

(c) Enhanced Image

Fig. 2. Blind deblurring of linear motion blurred image. (a) Blurred image of moving truck on the Brooklyn-Queens Expressway. (b) Image magnitude after GCD processing. (c) Enhanced image.

and, similarly two other polynomials $B_1(z_1, z_2)$ and $B_2(z_1, z_2)$ such that

$$D_1(z_1, z_2)B_1(z_1, z_2) + D_2(z_1, z_2)B_2(z_1, z_2) = \psi_2(z_2) \not\equiv 0. \tag{37}$$

In particular, for any $z_1 = \mu$, from (37) we also have

$$D_1(\mu, z_2)B_1(\mu, z_2) + D_2(\mu, z_2)B_2(\mu, z_2) = \psi_2(z_2) \tag{38}$$

and hence, if we let

$$\mathrm{GCD}\{D_1(\mu, z_2), D_2(\mu, z_2)\} \triangleq C(z_2) \tag{39}$$

then the polynomial $C(z_2)$ must be a factor of $\psi_2(z_2)$ for every choice of $z_1 = \mu$. Moreover, from (36)

$$D_1(\mu, z_2)A_1(\mu, z_2) + D_2(\mu, z_2)A_2(\mu, z_2) = \psi_1(\mu). \tag{40}$$

Since the left side of (40) vanishes at every root of the GCD polynomial $C(z_2)$ given by (39), the right side of (40) must also vanish, implying that every $z_1 = \mu$ for which $C(z_2)$ exists as a nontrivial polynomial in (39), has to be a zero of $\psi_1(z_1)$.

However, $\psi_1(z_1)$ only has a finite number of zeros, hence it follows that the GCD $C(z_2)$ in (39) can exist as a function of z_2 only for a finite number of values of z_1. In general, these finite number of special points will be arbitrarily located in the 2-D plane, hence it is reasonable to assume that the distinguished unit circles ($|z_1| = 1, |z_2| = 1$) are free of such points. Thus, for $\mu = e^{-j(2\pi m/M)}$, we will assume the GCD in (39) to be independent of z_2, justifying the approach in (26)–(28).

III. Experimental Results

Using simulated distorted images, the 2-D GCD approach is found to be efficient and reliable when SNR $\geq$ 40 dB. Fig. 1(b) and (c) are two blurred versions of a "lady with hat," obtained by convolving each of the R, G, and B channels of the original 146 $\times$ 128 image in Fig. 1(a) with two relatively co-prime 8 $\times$ 8 distortion filters and then adding uniform white noise so that SNR = 45 dB. Note that SNR is defined as the ratio of the signal variance to the noise variance [18]. The estimation using the above interpolative 2-D GCD approach is shown in Fig. 1(d). CPU time required to reconstruct each RGB channel in this case is approximately 4 min on a 143 MHz Sun Ultra running Matlab. The percentage MSE of the reconstruction is 0.32% in this case.

For the case when only one blurred image is available, when the support of the blurring function is small compared to the blurred image, the blurred image can be partitioned such that each part

completely contains the blurring function. In this case, the blurring function $D(z_1, z_2)$ becomes the GCD among these partitioned images, and the different parts of the original scene now serve as the co-prime multiplicative factors. A special case is linear motion blur, where the blurring function is 1-D. In this case, each line along the motion contains the same blurring function. Fig. 2(a) shows a blurred picture of letters taken from one frame of a video sequence of a fast moving truck. A Cannon Hi8 camcorder was used to provide a reasonably clear image sequence. The selected frame was then digitized, and the predominant red channel was used as a gray-level image. There are two blurred parts of letters on the image. The larger string on top is used to find the blurring function by averaging the GCD of two distant blurred lines. Then we restored the entire image area using the deduced blurring function. Fig. 2(b) shows the result of the above algorithm. Here, the large letters are clearly recognizable, and the smaller blurred string is also revealed to contain letters. Fig. 2(c) shows the reconstructed image after median filtering and enhancement. Notice that even the smaller string of letters at the bottom is now recognizable as "KING OF BEERS."

The approach described in this section is targeted toward fast 2-D GCD algorithms that are also robust. The robustness results from the fact that the rank conditions presented in the lemma in Section II, for example, can be formulated as a hypothesis testing problem for a given performance accuracy. Once the rank of its Sylvester matrix is determined by identifying a certain set of its smallest singular values as zeros, that gives the degree of the GCD and the desired polynomial approximations.

IV. Conclusions

This paper addresses the important, and often ill-posed, problem of blind image deconvolution by finding the "approximate" common factor (GCD) in presence of noise. With the assumption that the distortion filters are FIR and relatively co-prime, in the absence of noise, this becomes a problem of taking the greatest common divisor (GCD) of two or more 2-D polynomials. Exact GCD is not desirable because even extremely small variations due to quantization error or additive noise can destroy the integrity of the polynomial system and lead to a trivial solution. Our approach to this blind deconvolution approximation problem introduces a robust interpolative 2-D GCD method based on a 1-D Sylvester-type GCD algorithm.

The approach described here can be extended to the case when both the image and/or the blurring functions have infinite support. In that case, if the corresponding transfer functions are rational, then under relatively co-prime conditions for the numerator and denominator set of polynomials, the GCD approach can be separately applied to the numerator as well as the denominator pairs of the blurred images to recover the original image.

The problem of *simultaneously* obtaining the GCD of three or more polynomial functions is an interesting related problem, and a robust version of that algorithm is of practical importance as it corresponds to recovery from multiple blurred frames. To respect the simultaneous involvement of all polynomials, let $A(z)$, $B(z)$, and $C(z)$ represent three polynomials such that

$$\mathrm{GCD}\{A(z), B(z), C(z)\} = P(z). \tag{41}$$

In this case, to obtain the necessary and sufficient conditions that incorporate the coefficients of $A(z)$, $B(z)$, and $C(z)$ *simultaneously*, the classical approach considers the doublet [14]

$$\lambda A(z) + \mu B(z) \quad \text{and} \quad C(z) \tag{42}$$

where λ and μ are free variables. Clearly, the GCD of the triplet $A(z)$, $B(z)$, and $C(z)$, as well as the two polynomials in (42), are identical to $P(z)$ for *every* choice of the free variables λ and μ. Notice that the situation in (42) is algebraically the same as that in (13), hence it can be rewritten as in (16) and (17). However, the Sylvester matrix $S(\lambda, \mu)$ in this case is a function of λ and μ, and its singularity for *every* choice of λ and μ leads to vanishing coefficients of the two variable polynomial $\det S(\lambda, \mu)$. This results in complicated nonlinear conditions in terms of the original polynomial coefficients. It will be interesting to see whether such conditions can be organized in a more useful Sylvester-style matrix form.

On the other extreme, if only a single distorted image $f(n, m)$ is available, for the proposed procedure to work, it is important to generate at least two distinct blurred images from the given data. One-dimensional partitioning of images with linear motion blur is shown to be effective in our experiments [19], [20]. Real blurred pictures have been restored using such an approach, suggesting the practical value of the GCD blind image deconvolution algorithm.

References

[1] D. Kundur and D. Hatzinakos, "Blind image deconvolution," *IEEE Signal Processing Mag.*, May 1996, pp. 43–64.

[2] R. G. Lane and R. H. T. Bates, "Automatic multidimensional deconvolution," *J. Opt. Soc. Amer. A*, vol. 4, pp. 180–188, Jan. 1987.

[3] P. J. Bones, C. R. Parker, B. L. Satherley, and R. W. Watson, "Deconvolution and phase retrieval with use of zero sheets," *J. Opt. Soc. Amer. A*, vol. 12, pp. 1842–1857, Sept. 1995.

[4] D. C. Ghiglia, L. A. Romero, and G. A. Mastin, "Systematic approach to two-dimensional blind deconvolution by zero-sheet separation," *J. Opt. Soc. Amer. A*, vol. 10, pp. 1024–1036, May 1993.

[5] R. L. Lagendijk, A. M. Tekalp, and J. Biemond, "Maximum likelihood image and blur identification: A unifying approach," *Opt. Eng.*, vol. 29, pp. 422–435, May 1990.

[6] S. J. Reeves and R. M. Mersereau, "Blur identification by the method of generalized cross-validation," *IEEE Trans. Image Processing*, vol. 1, pp. 301–311, July 1992.

[7] G. R. Ayers and J. C. Dainty, "Iterative blind deconvolution method and its applications," *Opt. Lett.*, vol. 13, pp. 547–549, July 1988.

[8] B. C. McCallum, "Blind deconvolution by simulated annealing," *Opt. Commun.*, vol. 75, pp. 101–105, Feb. 1990.

[9] D. Kundur and D. Hatzinakos, "A novel recursive filtering method for blind image restoration," in *Proc. IASTED Int. Conf. on Signal and Image Processing*, Nov. 1995, pp. 428–431.

[10] H. S. Wu, "Minimum entropy deconvolution for restoration of blurred two-tone images," *Electron. Lett.*, vol. 26, pp. 1183–1184, July 1990.

[11] G. Harikumar and Y. Bresler, "Efficient algorithms for the blind recovery of images blurred by multiple filters," in *Proc. IEEE Int. Conf. Image Processing*, Sept. 1996, vol. III, pp. 97–100.

[12] G. B. Giannakis and R. W. Heath, Jr., "Blind identification of multichannel FIR blurs and perfect image restoration," in *Proc. IEEE Int. Conf. Image Processing*, Sept. 1996, vol. I, pp. 717–720.

[13] G. Xu, H. Liu, L. Tong, and T. Kailath, "A least-squares approach to blind channel identification," *IEEE Trans. Signal Processing*, vol. 43, pp. 2982–2993, Dec. 1995.

[14] M. Bocher, *Introduction to Higher Algebra*. New York: MacMillan, 1959.

[15] D. V. Chudnovsky and G. V. Chudnovsky, "Computer algebra in the service of mathematical physics and number theory," *Computers in Mathematics*. New York: Marcel Dekker, 1990, pp. 109–232.

[16] E. Kaltofen, "Polynomial factorization 1982–1986," *Computers in Mathematics*. New York: Marcel Dekker, 1990, pp. 285–310.

[17] D. Knuth, "The analysis of algorithms," *Actes Congrés. Intern. Math.*, vol. 3, pp. 269–274, 1970.

[18] M. R. Banham and A. K. Katsaggelos, "Digital image restoration," *IEEE Signal Processing Mag.*, pp. 24–41, Mar. 1997.

[19] S. U. Pillai, "Blind image recovery from a single image," Int. Rep., Polytechnic Univ., Brooklyn, NY, 1996.

[20] B. Liang, "Blind image deconvolution and a robust GCD approach," M.S. thesis, Polytechnic Univ., Brooklyn, NY, June 1997.